BBA - Molecular Basis of Disease 1865 (2019) 2083–2093

Contents lists available at ScienceDirect

BBA - Molecular Basis of Disease

journal homepage: www.elsevier.com/locate/bbadis

A mouse model for intellectual disability caused by mutations in the X-linked 2′-*O*-methyltransferase *Ftsj1* gene

Lars R. Jensen[a,*], Lillian Garrett[b,c], Sabine M. Hölter[b,c], Birgit Rathkolb[b,d,e], Ildikó Rácz[b,f,g], Thure Adler[b], Cornelia Prehn[b], Wolfgang Hans[b], Jan Rozman[b,e], Lore Becker[b], Juan Antonio Aguilar-Pimentel[b], Oliver Puk[c], Kristin Moreth[b], Monika Dopatka[h], Diego J. Walther[i], Viola von Bohlen und Halbach[j], Matthias Rath[k,ac], Martin Delatycki[l], Bettina Bert[m], Heidrun Fink[m], Katharina Blümlein[n], Markus Ralser[o], Anke Van Dijck[p,q], Frank Kooy[p], Zornitza Stark[l], Sabine Müller[r], Harry Scherthan[s], Jozef Gecz[t,ad], Wolfgang Wurst[c,u,v,w], Eckhard Wolf[d], Andreas Zimmer[f], Martin Klingenspor[x,y], Jochen Graw[c], Thomas Klopstock[v,w,z], Dirk Busch[aa], Jerzy Adamski[b,ab], Helmut Fuchs[b], Valérie Gailus-Durner[b], Martin Hrabě de Angelis[b,e,ab], Oliver von Bohlen und Halbach[j], Hans-Hilger Ropers[i], Andreas W. Kuss[a,*]

[a] *Department of Functional Genomics, Interfaculty Institute of Genetics and Functional Genomics, University Medicine Greifswald, Felix-Hausdorff-Strasse 8, 17489 Greifswald, Germany*
[b] *German Mouse Clinic, Helmholtz Zentrum München, German Research Center for Environmental Health, Neuherberg, Germany*
[c] *Institute of Developmental Genetics, Helmholtz Zentrum München, German Research Center for Environmental Health, Ingolstädter Landstrasse 1, 85764 Neuherberg, Germany*
[d] *Institute of Molecular Animal Breeding and Biotechnology, Gene Center, Ludwig-Maximilians-University München, Feodor-Lynen Str. 25, 81377 München, Germany*
[e] *German Center for Diabetes Research (DZD), Ingolstädter Landstr. 1, 85764 Neuherberg, Germany*
[f] *Institute of Molecular Psychiatry, Medical Faculty, University of Bonn, Sigmund Freud Str. 25, 53127 Bonn, Germany*
[g] *Clinic of Neurodegenerative Diseases and Gerontopsychiatry, University of Bonn Medical Center, Bonn, Germany*
[h] *Department of Experimental Neurology, Charite, Berlin, Germany*
[i] *Max Planck Institute for Molecular Genetics, Berlin, Germany*
[j] *Institute of Anatomy and Cell Biology, University Medicine Greifswald, Greifswald, Germany*
[k] *Department of Human Genetics, University Medicine Greifswald, Greifswald, Germany*
[l] *Bruce Lefroy Centre for Genetic Health Research, Murdoch Children's Research Institute, Victoria, Australia*
[m] *Institute for Pharmacology and Toxicology, FB Veterinary Medicine, Free University, Berlin, Germany*
[n] *Fraunhofer Institute for Toxicology and Experimental Medicine, Hannover, Germany*
[o] *Molecular Biology of Metabolism Laboratory, The Francis Crick Institute, 1 Midland Road, London NW1 1AT, UK*
[p] *University of Antwerp, Department of Neurology - Antwerp University Hospital, Edegem, Belgium*
[q] *Department of Medical Genetics, University of Antwerp, Antwerp, Belgium*
[r] *Institute of Biochemistry, University Greifswald, Greifswald, Germany*
[s] *Bundeswehr Institute of Radiobiology affiliated to the University of Ulm, Munich, Germany*
[t] *School of Medicine, Robinson Research Institute, University of Adelaide, Adelaide, SA 5000, Australia*
[u] *Technische Universität München, Freising-Weihenstephan, Germany*
[v] *Deutsches Institut für Neurodegenerative Erkrankungen (DZNE), Site Munich, 80336 München, Germany*
[w] *Munich Cluster for Systems Neurology (SyNergy), Adolf-Butenandt-Institut, Ludwig-Maximilians-Universität München, Schillerstr. 44, 80336 München, Germany*
[x] *Technical University Munich, EKFZ – Else Kröner Fresenius Center for Nutritional Medicine, Gregor-Mendel-Str. 2, 85350 Freising-Weihenstephan, Germany*
[y] *ZIEL – Institute for Food and Health, Technical University Munich, Gregor-Mendel-Str. 2, 85350 Freising-Weihenstephan, Germany*
[z] *Department of Neurology, Friedrich-Baur-Institute, Klinikum der Ludwig-Maximilians-Universität München, Ziemssenstr. 1a, 80336 München, Germany*
[aa] *Institute for Medical Microbiology, Immunology and Hygiene, Technische Universität München, Trogerstrasse 30, 81675 Munich, Germany*
[ab] *School of Life Science Weihenstephan, Technische Universität München, Alte Akademie 8, 85354 Freising, Germany*
[ac] *Interfaculty Institute of Genetics and Functional Genomics, University of Greifswald, Greifswald, Germany*
[ad] *South Australian Health and Medical Research Institute, Adelaide, SA 5000, Australia*

* Corresponding authors.
E-mail address: jensenl@uni-greifswald.de (L.R. Jensen).

https://doi.org/10.1016/j.bbadis.2018.12.011
Received 6 July 2018; Received in revised form 6 December 2018; Accepted 10 December 2018
Available online 14 December 2018
0925-4439/ © 2019 The Authors. Published by Elsevier B.V. This is an open access article under the CC BY license (http://creativecommons.org/licenses/BY/4.0/).

ARTICLE INFO

Keywords:
Ftsj1
tRNA methyltransferase
Intellectual disability
X-linked
Mouse model

ABSTRACT

Mutations in the X chromosomal tRNA 2′-*O*-methyltransferase FTSJ1 cause intellectual disability (ID). Although the gene is ubiquitously expressed affected individuals present no consistent clinical features beyond ID. In order to study the pathological mechanism involved in the aetiology of *FTSJ1* deficiency-related cognitive impairment, we generated and characterized an *Ftsj1* deficient mouse line based on the gene trapped stem cell line RRD143. Apart from an impaired learning capacity these mice presented with several statistically significantly altered features related to behaviour, pain sensing, bone and energy metabolism, the immune and the hormone system as well as gene expression. These findings show that *Ftsj1* deficiency in mammals is not phenotypically restricted to the brain but affects various organ systems. Re-examination of ID patients with *FTSJ1* mutations from two previously reported families showed that several features observed in the mouse model were recapitulated in some of the patients. Though the clinical spectrum related to *Ftsj1* deficiency in mouse and man is variable, we suggest that an increased pain threshold may be more common in patients with *FTSJ1* deficiency. Our findings demonstrate novel roles for *Ftsj1* in maintaining proper cellular and tissue functions in a mammalian organism.

1. Introduction

Intellectual disability (ID) is defined by significant limitations in intellectual performance (intelligence quotient < 70) and a reduction of conceptual, social and practical skills with an onset before the age of 18. ID is a major developmental disorder and currently ID is estimated to affect around 1% of the general population, but with large regional differences [1]. Historically ID was separated into syndromic and non-syndromic forms, with the former being ID in the presence of clinically consistent features. The non-syndromic forms seem more common, but as more patients with similar gene defects are molecularly diagnosed syndromic features may become apparent.

Although ID has genetic as well as environmental causes (like excessive alcohol consumption during pregnancy), severe forms are often caused by genetic defects in single genes [2–4].

Monogenic recessive causes of ID have been excessively studied in X-linked forms and with the development of next-generation-sequencing techniques the elucidation of autosomal forms has also made a leap forward. Mutation discovery studies so far have clearly shown that ID is genetically and functionally heterogeneous but also that several ID proteins interact, are involved in the same process or target the same substrate. One emerging “ID gene group” is involved in tRNA modifications and includes *NSUN2* [5–7], *ADAT3* [8], *TRMT10A* [9,10], *TRIT1* [11], *TRMT1* [3], *ELP2* [3,12], *PUS3* [13], *MTO1* [14] and *FTSJ1* [15–18].

ID-causing mutations affecting *FTSJ1* are mainly loss-of-function variants that prematurely truncate the protein by affecting splicing or directly introduce stop-codons, while more recently an *FTSJ1* missense mutation was detected in an ID patient [19].

FTSJ1 encodes a ubiquitously expressed and evolutionarily highly conserved 2′-*O*-methyltransferase that uses S-adenosylmethionine as methyl donor [20]. Mammalian FTSJ1 is not as well characterized as its yeast homologue, but the function is highly conserved as human FTSJ1 is able to methylate yeast $tRNA^{Phe}$ at position 32 and 34 in yeast cells [21]. 2′-*O*-methylation of $tRNA^{Phe}$ also appears to be its major target [21] and yeast cells deficient in the Ftsj1 homologue Trm7 grow slowly and show reduced mRNA translation [20]. Trm7 methylates $tRNA^{Phe}$, $tRNA^{Trp}$ and $tRNA^{Leu(UAA)}$ at position C_{32} and N_{34} [20] using two different protein interaction partners, TRM732 and TRM734, which are required for each modification [20–22]. Both modifications are required for the subsequent conversion of 1-methylguanosine at position 37 to wyebutosine in $tRNA^{Phe}$ [22].

Still, mammalian FTSJ1 is largely uncharacterized and the consequences of *FTSJ1* deficiency in human seem to mainly affect cognition. Therefore, in order to study the effect of *FTSJ1* deficiency not only on brain function but also on other organs, we set out to generate *Ftsj1* deficient mice. Here we report the results of a thorough characterization of our mouse model, showing that in addition to alterations in learning and memory other features including nociception, metabolism, hormone levels and the immune system are affected, some of which could also be found in human carriers of deleterious *FTSJ1* mutations that are affected with ID.

2. Materials and methods

2.1. Generation of Ftsj1 deficient mice

Ftsj1 gene trapped mice were generated by microinjection of gene trapped ES-cells. The mouse embryonic stem cell line RRD143 (129P2/OlaHsd) containing a gene trap insertion in intron 5 of the *Ftsj1* gene was obtained from Baygenomics and expanded on a layer of cell division deficient mouse embryonic feeder cells. Blastocysts were obtained from hormonally stimulated (superovulating) female C57BL/6J mice. The round and smooth ES-cells were injected into the blastocyst cavity and surgically transferred into pseudo-pregnant recipient female mice using standard methods, essentially as described [49]. Chimeric pups were identified by the presence of brown coat spots and bred to select for germline transmission. Offspring harboring gene trapped *Ftsj1* were then backcrossed to a C57BL/6J genetic background for at least 10 generations before they were expanded to provide wild type and gene trapped littermates of both sexes for phenotypic characterization. In this process we also removed other gene traps that could have been integrated in the genomic DNA during the RRD143 cell line generation. For the mouse characterization at the German Mouse Clinic (www.mouseclinic.de) a cohort of 54 animals were used. 12 $Ftsj1^{-/y}$ males, 15 control males, 12 $Ftsj1^{-/-}$ females and 15 $Ftsj1^{-/x}$ control female mice were born within one week from the mating of hemizygous *Ftsj1* gene trapped males with heterozygous females.

All tests performed at the GMC were approved by the responsible authority of the district government of Upper Bavaria, Germany. The hole-board test was carried out according to the guidelines of the Landesamt für Landwirtschaft, Lebensmittelsicherheit und Fischerei (LALLF) Mecklenburg-Vorpommern, Germany.

2.2. RT-PCR and PCR

Total RNA was isolated from cultured cells or mouse tissues using TRIzol (Life Technologies, Carlsbad, CA, USA) according to the manufacturer's instructions. RNA integrity was verified on ethidium bromide stained agarose gels. For cDNA synthesis 1 μg total RNA was reverse transcribed using random priming and Superscript III (Life Technologies, Carlsbad, CA, USA) according to the manufacturer's instructions. cDNA corresponding to 20 ng total RNA was amplified using the GoTaq G2 Colorless Master Mix (Promega, Madison, WI, USA). For RT-PCR we used the primers: FTSJ1_5UTR_U 5′-ATACGTTGTGCTCCG GTCTG-3′ and FTSJ1_ex7-8L 5′-ATATCTTGGCCACGAAGCAG-3′ for detecting a 705 bp wild type *Ftsj1* PCR product and the primers mm_FTSJ1_GT1u1 5′-GTGCTGAGCCAGAAGGTTG-3′ and

mm_FTSJ1_GT1l1 5′-GGCGATTAAGTTGGGTAACG-3′ for detecting a 352 bp PCR product containing a part of *Ftsj1* and the gene trap sequence. As ladder the pUC Mix Marker 8 (MBI Fermentas #SM 0302, St Leon-Rot, Germany) was used.

2.3. Genotyping by PCR

Mouse genomic DNA was isolated from tail or ear tissue using the NucleoSpin Tissue kit (Macherey & Nagel, Düren, Germany) following the manufacturer's instructions. The DNA concentration was measured with a QuBit fluorometer (Life Technologies, Carlsbad, CA, USA). 20 ng DNA was amplified by PCR with primer combinations specific for the wild type *Ftsj1* or for the gene trapped *Ftsj1*, respectively. One oligonucleotide was used for both PCRs mm_FTSJ1_GT1u3 5′-TCTGACCAC ACGTTGTGTTG-3′ in combination with Ftsj1_in5_1l3 5′-AAGAAGAGT GTCAGATCCTCTG-3′ to obtain a 531 bp product for the wild type sequence, and oligonucleotide pGT1lxf_4l1 5′-AGGGAAAGGGTAAAGTG GTAG-3′ for detecting the gene trap in a PCR product of 240 bp.

2.4. Phenotyping

At the German Mouse Clinic (GMC) the mice were subjected to an extensive phenotypic screening, including standardized phenotyping in the areas of dysmorphology, behaviour, neurology, nociception, energy metabolism, clinical chemistry, cardiovascular features, eye, lung function, molecular features, immunology, steroid metabolism and pathology [50,51] (see also www.mouseclinic.de). The phenotypic tests were part of the GMC screen, which were performed according to standardized protocols as described [52,53]. The experiments were not in general blinded. However, the preparation and organization of the experimental procedures at the German Mouse Clinic are adapted in a tailor-made way for each single test according to the specific requirements. When applicable, tests and analyses were carried out by an automated system where the experimenter had no influence on the outcome of the test (*e.g.* acoustic startle and prepulse inhibition, open field test, blood based parameters and DEXA analysis). When tests were carried out in parallel with a subset of the animals (*e.g.* indirect calorimetry, open field test, acoustic startle and prepulse inhibition), mutant and control animals were distributed either in a random or in a balanced way between the different apparatuses. Meta data for experimental conditions were recorded and analyzed for deviations.

The hole-board test was performed as described [54] using mice from three litters in total consisting of 6 gene trapped and 7 control male mice.

2.5. Statistical analyses

About 500 parameters belonging to 14 different disease areas were measured during the primary GMC screen. As level of significance for statistical analyses of GMC-screening results we used a p-value < 0.05 (without correction for multiple testing). If not stated otherwise, data generated by the German Mouse Clinic were analyzed using R. Tests for genotype effects were made by using *t*-test, Wilcoxon rank sum test, linear models, or ANOVA depending on the assumed distribution of the parameter and the questions addressed to the data.

2.6. mRNA expression profiling

Brain tissue was obtained from mice from 3 litter pairs that were 7, 9 and 14 months old, each consisting of one wt male and one hemizygous gene trapped male. We chose to use littermates of different age because the effects of *FTSJ1* deficiency seem to be constant over time in human patients as no improvement in cognition has been reported. By sequencing and analyzing data from the mice separately we obtain information on expression differences between gene trapped and wildtype mice at different age, while still having the option to pool data from gene trapped and control mice, respectively. The tissue was homogenized using a polytron device (VWR) in the presence of TRIzol reagent (Life Technologies, Carlsbad, CA, USA) according to the instructions of the manufacturer. Next, we removed the rRNA from the RNA samples using a RiboZero Kit (Epicentre, Madison, WI, USA) according to the manufacturers' instructions and spiked the RNA with ERCC RNA Spike-in Mix (Life Technologies, Carlsbad, CA, USA). The RNA was fragmented by chemical hydrolysis, phosphorylated and purified. Adaptors were then ligated to the RNA fragments and reverse-transcribed into cDNA. The cDNA was then further processed to sequencing libraries using recommended protocols and chemicals, which were then paired-end sequenced (75 nucleotides in the forward direction and 35 nucleotides in the reverse direction) using a SOLiD 5500xl Genetic Analyzer (Life Technologies, Carlsbad, CA, USA). For mapping of the sequence reads we used the GRCm38/mm10 assembly sequence build (ftp://hgdownload.cse.ucsc.edu/goldenPath/mm10/) as a

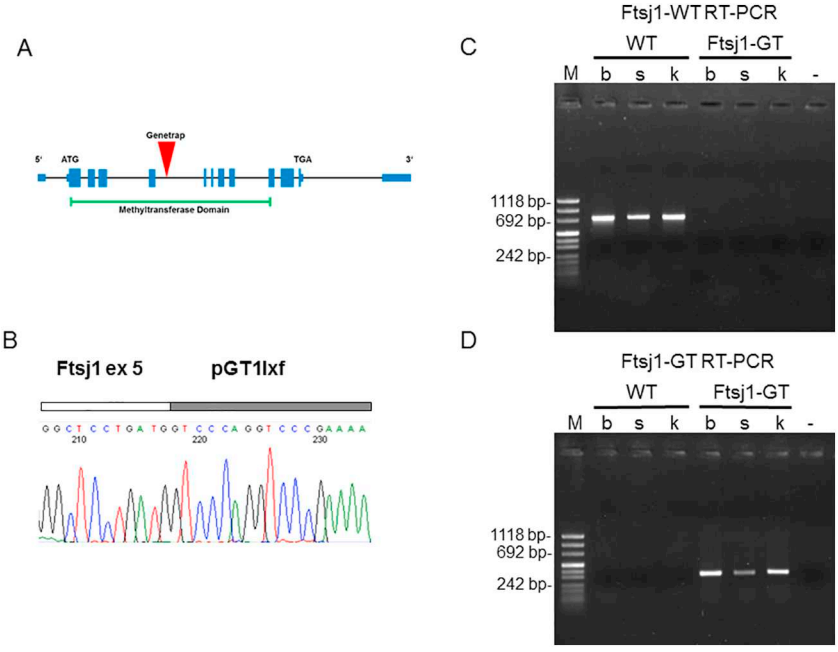


Fig. 1. The gene trap efficiently traps Ftsj1 transcripts in the gene trapped mice. (A) Schematic representation of the *Ftsj1* gene and position of the gene trap insertion. (B) Sequence chromatogram showing that the gene trap is part of the Ftsj1 transcript in Ftsj1 gene trapped (Ftsj1-GT) mice. (C) Agarose gel showing RT-PCR products obtained from mouse brain (b), spleen (s) and kidney (k) generated with primers specific for Ftsj1 wild type transcript. Note that there is no detectable wild type transcript in the Ftsj1 gene trapped mice. (D) RT-PCR using primers specific for the gene trapped allele. WT: Wild type mice; Ftsj1-GT: gene trapped mice; M: pUC Mix Marker 8 DNA ladder.

reference and followed the workflow 'whole.transcriptome.pe' of LifeScope-v2.5.1-r0 (Life Technologies, Carlsbad, USA). Of these we considered sequence reads that mapped to RefSeq coding exons (http://hgdownload.cse.ucsc.edu/goldenPath/mm10/database/refGene.txt.gz) and matched the coding strand to be coding RNAs. All other reads were considered to be non-coding. Differential expression analysis was performed as previously described [55]. In brief, reads were normalized for GC-content using EDASeq's full quantile normalization [56] and the differential expression analysis was carried out using DESeq [57]. All data were treated as replicates of a single condition. The significance of the differential expression values was determined using Benjamini-Hochberg corrected p-values between two conditions (control or gene trapped mice) with the significance threshold set to 0.05.

2.7. Patient reexamination

Our studies of the molecular background of cognitive disorders are approved by the ethical committee of the University Medicine Greifswald. Clinical examinations were performed with the consent of the affected Individuals and/or their legal guardians. All methods were carried out in accordance with relevant guidelines and regulations.

3. Results

3.1. Validation of the gene trap in cells and mice

By PCR amplification of genomic DNA extracted from the mouse embryonic stem cell line RRD143 and subsequent Sanger sequencing of the PCR products we identified the exact location of the gene trap in intron 5 of the *Ftsj1* gene (ChrX: 7,825,518 and 7,825,539) corresponding to position c.361 + 566 to c.361 + 587 at the cDNA level (mouse NCBI37/mm9). After generating the gene trapped mice we extracted RNA from brain, spleen and kidney and could show by RT-PCR that the gene trap is part of the *Ftsj1* transcript, effectively generating an *Ftsj1* deficient mouse line as no wild-type transcript was visible in these tissues (Fig. 1). As human female heterozygous *FTSJ1* mutation carriers are affected to a much lesser extent than male hemizygous carriers, we chose to compare homozygously gene trapped female mice with heterozygous female control mice.

3.2. Morphological features, body composition and energy metabolism

As expected for a mouse model for non-syndromic intellectual disability we did not observe genotype specific anatomical differences or differences in organ weight when normalized to body weight. Also no genotype effect on tibia length was observed and there was no association between genotype and the occurrence of anterior segment abnormalities, axial eye length, or altered visual properties. However, our preliminary observation that *Ftsj1* deficient mice are lighter ($p < 0.001$ for males and females) and shorter ($p < 0.001$ for males and $p = 0.017$ for females) was confirmed (Table 1). In addition, we found that fat mass and lean mass were significantly decreased in male gene trapped mice even though food intake was comparable for all genotypes. Using Dual-energy X-ray absorptiometry (DEXA) we found that relative body fat content was increased in gene trapped male mice whereas the lean mass was lower (Table 1), a difference that was attenuated over time (data not shown). Bone mineral content (BMC) and bone content (% of total weight) was significantly reduced in the gene trapped mice ($p < 0.001$) but without affecting bone mineral density (BMD, Table 1). Energy turnover and body temperature was not significantly changed and lactate levels and lactate dehydrogenase activity were also within the normal range (Supplementary Fig. 1).

3.3. Altered behaviour and nociception in Ftsj1 deficient mice

To investigate behavioural changes in *Ftsj1* gene trapped mice, we

Table 1
Gene trapped mice are small and have reduced body weight and bone content.

	Female control N = 14	Female mutant N = 8	Male control N = 16	Male mutant N = 13	Pairwise (Tukey) females		Pairwise (Tukey) males		ANOVA	ANOVA	ANOVA
					Mutant-control		Mutant-control		Genotype	Sex	Sex: genotype
	Mean ± sd	Mean ± sd	Mean ± sd	Mean ± sd	Adj. p-value		Adj. p-value		p-Value	p-Value	p-Value
BMD[a] [mg/cm^2]	47 ± 4	49 ± 5	51 ± 4	50 ± 4	0.457		0.882		0.698	0.013	0.115
BMC[b] [mg]	308 ± 53	156 ± 48	378 ± 125	155 ± 70	0.001		< 0.001		< 0.001	0.292	0.158
Bone content [%]	1.29 ± 0.18	0.78 ± 0.23	1.25 ± 0.38	0.70 ± 0.30	0.001		< 0.001		< 0.001	0.216	0.777
Body length [cm]	9.41 ± 0.21	9.11 ± 0.31	9.61 ± 0.19	9.22 ± 0.18	0.017		< 0.001		< 0.001	0.027	0.449
Body weight [g]	23.83 ± 1.49	19.93 ± 1.62	30.7 ± 2.22	22.17 ± 1.44	< 0.001		< 0.001		< 0.001	< 0.001	< 0.001
Fat mass [g]	1.87 ± 1.08	0.55 ± 0.94	4.73 ± 2.68	0.40 ± 0.98	0.326		< 0.001		< 0.001	0.006	0.004
Lean mass [g]	17.24 ± 1.43	15.06 ± 1.84	20.14 ± 2.27	17.59 ± 1.66	0.05		0.003		< 0.001	< 0.001	0.732

[a] BMD: bone mass density.
[b] BMC: bone mass content.

subjected the animals to the following tests: open field test, Y-maze, social discrimination, prepulse inhibition/acoustic startle, place learning/reversal learning, grip strength, rotarod, hole-board and hot plate test.

In the open field test we observed a slightly decreased rearing activity ($p < 0.05$) among the homozygous mutant females when compared to the heterozygous controls, but neither the Y-maze nor the social discrimination test showed consistent differences between mutant and control mice (Supplementary Table 1). Only *Ftsj1* gene trapped males showed decreased acoustic startle activity (after body weight normalization, $F_{(7,196)} = 4.584$, $p < 0.001$), but no change in prepulse inhibition (Supplementary Table 1). Place and reversal learning as evaluated by using the IntelliCage system, however, was significantly impaired in male mutants (Fig. 2).

Interestingly, heterozygous females showed a significantly increased error rate in place learnig during the first and the third day, but the significance level was not reached any more during the following sessions and reversal learning did not show differences between female heterozygotes and female homozygous wild type mice (not shown). Muscle function was assessed through grip strength tests, which showed reduced strength for the male gene trapped mice. However, after normalizing for the lower body weight observed for the gene trapped mice, only the forelimb grip strength was statistically significant (Fig. 3H). The reduced muscle strength did not affect motor coordination as the rotarod test did not show genotype specific differences (Supplementary Table 1). Using the hole-board test we observed that male gene trapped mice dipped the head through the opening more often than control mice ($p = 0.005$) suggesting a more explorative/less anxious behaviour as compared to controls. The total distance traveled and rearing behaviour was not statistically different between the two groups (Supplementary Table 1).

We used the hot plate test to investigate the response to a thermal pain stimulus and found that gene trapped male mice as well as homozygous gene trapped females show hypoalgesia. The latency time was significantly longer for both the first ($p = 0.007$) and the second reaction ($p < 0.001$). There were no differences in the type of reaction to the stimuli or in hind paw shaking or hind paw licking (Fig. 2).

3.4. Altered metabolism in Ftsj1 deficient mice

We observed that the loss in body weight after overnight fasting was relatively larger for the Ftsj1 deficient males as compared to the male controls ($p < 0.001$). The heterozygous females showed the same trend, but not as pronounced ($p < 0.05$). We observed lower glucose levels both in *ad libitum* fed and fasted male gene trapped mice. In the intraperitoneal Glucose Tolerance Test (IpGTT) we furthermore found lower AUC 0–30 (Fig. 3) and AUC 30–120 values in male gene trapped mice suggesting that they were significantly better at clearing intraperitoneally injected glucose from the bloodstream ($p < 0.001$). This indicates an improved glucose tolerance in the male gene trapped mice.

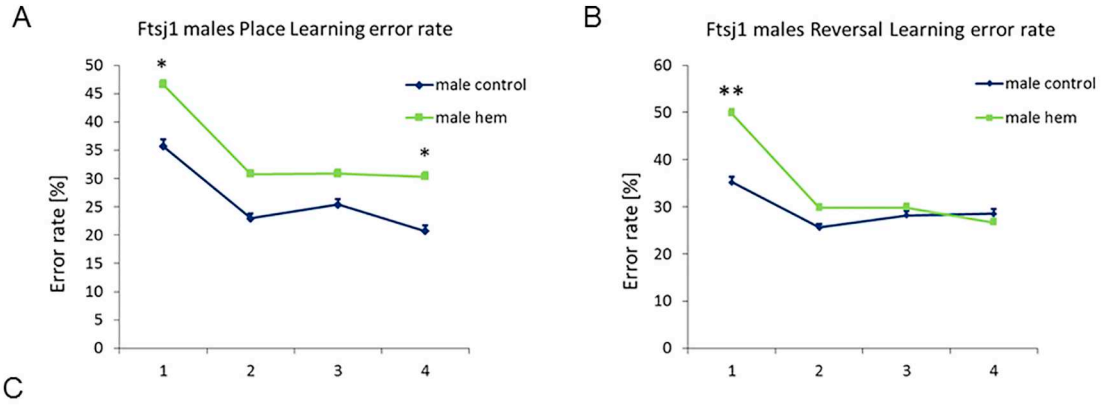
Further clinical chemistry analysis revealed decreased cholesterol and triglyceride levels in fasted and *ad libitum* fed mutant male mice. Both HDL and non-HDL cholesterol was similarly affected in the fasted animals (not shown). In the *ad libitum* fed state we also found decreased total protein and creatinine levels and decreased alpha-amylase activity in gene trapped male mice (Fig. 3). We also observed a trend towards lower iron levels and higher alkaline phosphatase (ALP) activity ($p = 0.008$, Supplementary Fig. 1). Only in male gene trap carriers we saw slightly decreased sodium ($p = 0.04$) and calcium ($p = 0.011$, Supplementary Fig. 1) levels.

3.5. Hematology, immune system and steroid metabolism

Through a hematological analysis we observed slightly more red blood cells in gene trapped male mice ($p = 0.084$) than in the controls. The hematocrit values were not affected but the mean corpuscular volume was significantly decreased ($p < 0.001$) suggesting mild microcytosis. The red blood cell distribution width (RDW) was slightly higher in mutant mice ($p = 0.005$) suggesting increased anisocytosis in these animals. The effects were more pronounced in the male mice.

The mean corpuscular hemoglobin (MCH) was significantly decreased in mutant animals ($p < 0.001$) but the cellular hemoglobin concentration (MCHC) was not significantly affected.

The platelet count (PLT) showed a significant reduction in the gene



C

	mean ± sd	mean ± sd	mean ± sd	mean ± sd	pairwise (Tukey)	pairwise (Tukey)	ANOVA	ANOVA	ANOVA
	female	female	male	male	females	males			
	control	mutant	control	mutant	mutant-control	mutant-control	genotype	sex	sex: genotype
	N=16	N=12	N=16	N=14	adj. p-value	adj. p-value	p-value	p-value	p-value
First response time	14.33 ± 4.42	18.14 ± 6.45	13.96 ± 3.56	17.52 ± 5.49	0,198	0,216	0,007	0,793	0,926
Second response time	23.31 ± 4.82	29.19 ± 1.24	22.24 ± 4.55	28.56 ± 2.94	0,001	< 0.001	< 0.001	0,525	0,831

Fig. 2. Place learning, reversal learning and nociception is impaired in Ftsj1 gene trapped mice. (A) Place learning and (B) reversal learning error rate for male mutant and control mice on four different consecutive days. (C) Ftsj1 gene trapped male and female mice have elevated pain threshold as measured by the (prolonged) response time to a thermal stimulus. sd: Standard deviation, ANOVA: analysis of variance results.

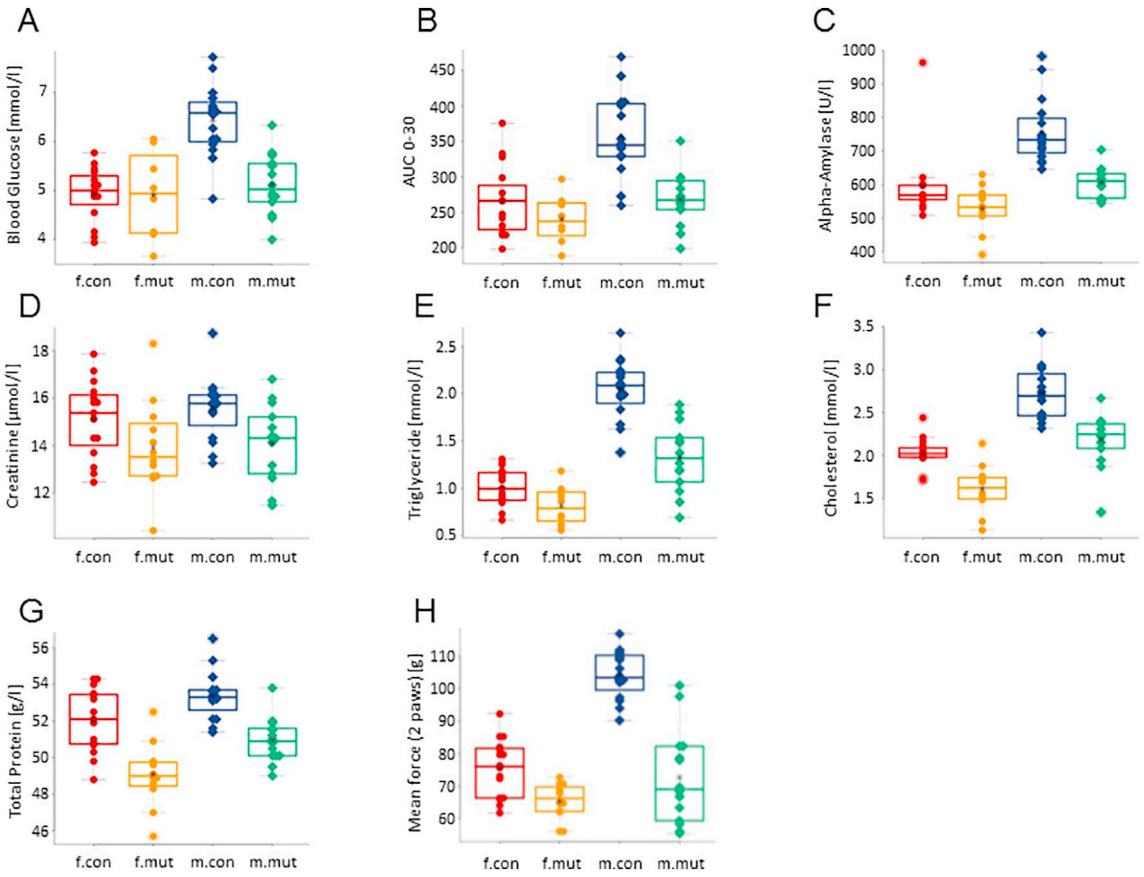


Fig. 3. Blood glucose, metabolite levels and grip strength are reduced in Ftsj1 deficient male mice. Blood glucose concentration is lower in gene trapped mice as compared to wild type male mice (A). Injected glucose is cleared faster from the blood in gene trapped male mice as compared to wild type male mice. Shown are area under curve values for the first 30 min of the test (AUC 0–30 min) (B). Alpha-amylase (C), creatinine (D), triglycerides (E), cholesterol (F), total protein concentration (G) and grip strength (H) are reduced in male gene trapped mice. Female mice show the same trend as male mice, but less pronounced. The data are presented as box plot with strip charts showing the individual animals split by sex and genotype. Female mice are shown as filled circles and males as diamonds. The box represents the 25% and 75% quartile and the line within the boxplot represents the median. The asterisk represents the mean. Circled points or diamonds denote values outside 1.5× the interquartile range. f.con: female Ftsj1$^{+/-}$ mice (n = 15); f.mut: female Ftsj1$^{-/-}$ mice (n = 12); m.con: male Ftsj1$^{+/y}$ mice (n = 16); m.mut: male Ftsj1$^{-/y}$ mice (n = 14). Data were analyzed using a linear regression model.

trapped mice ($p = 0.003$) and the mean platelet volume was also reduced in these animals ($p = 0.019$) whereas the platelet distribution width (PDW) was not affected.

We also found a higher white blood cell count in gene trap carriers ($p = 0.01$) of both sexes and measured the leukocyte subpopulation frequencies. We observed a reduced proportion of CD25 expressing CD4+ T cells in male and female mutant mice ($p < 0.001$).

Within the B cell compartment, we observed lower frequencies of IgD (female: $p = 0.021$, male $p = 0.013$) and MHC class II expressing cells (female: $p = 0.04$, male: $p < 0.001$). In male mutants we furthermore found a slight increase in granulocytes ($p = 0.021$) and a slight decrease in B cell frequency ($p = 0.027$). However, in the allergy screen, we found no differences in IgE levels between mutant and control mice, suggesting an absence of allergy or autoimmune responses as the level of autoantibodies was in the zero-range (not shown).

Measuring IgG in blood plasma we found less IgG1 in male ($p < 0.001$), but not in female mutant animals and less IgG3 in female ($p = 0.023$) but not in male mutant mice. Finally, we measured the levels of three steroids in blood plasma: corticosterone, testosterone and androstenedione. Testosterone and androstenedione were within normal range but corticosterone levels were significantly increased in male and female gene trap carriers ($p < 0.001$, Fig. 4).

3.6. RNA expression profiling

We extracted RNA from the whole brain of 3 male wt and 3 male gene trapped mice and prepared libraries that were sequenced on a SOLiD 5500xl machine. After read-mapping to the mouse genome (GRCm38/mm10 assembly), expression profiles were generated. We found that *Ftsj1* expression in gene trapped mice was reduced to 15 to 21% of the levels observed in unaffected littermates. However, almost all of the reads in the gene trapped mice were located between the transcription start site and the gene trap (located between exon 5 and 6) whereas almost no reads were found between the gene trap and the 3′ end of the gene. This result is in line with the RT-PCR analysis (see above) and confirms that gene trapped mice do not express detectable full length Ftsj1.

We then compared expression profiles of the three gene trapped mice with that of the three control mice and obtained 50 transcripts with an adjusted p-value < 0.05 (Table 2). Of these genes 39 code for proteins, which were functionally analyzed using the DAVID 6.8 software [23,24]. Based on the Gene Ontology (GO) annotation we found enrichment for genes belonging to the category “Biological processes” (BP), “Cellular compartment” (CC) and “Molecular function” (MF) (Supplementary Table 2). The two most significant entries from each

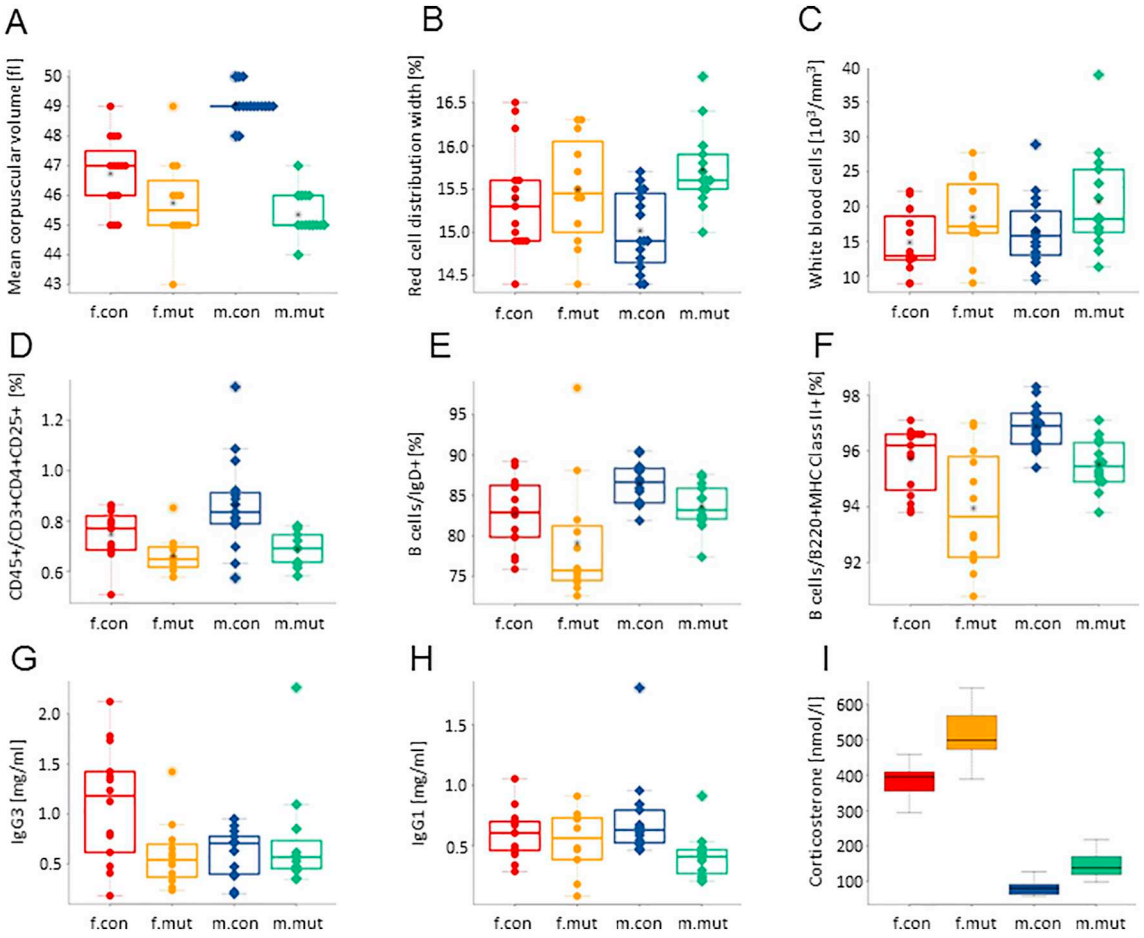


Fig. 4. Hematological, immunological and hormonal alterations in Ftsj1 gene trapped mice. The red blood cell mean corpuscular volume was reduced in mutant mice (A) and less equal in size (B) whereas the white blood cell count was increased in mutant mice (C). We also observed reduced proportions of $CD45^+$/CD3-CD4-CD25 expressing T-cells (D) and IgD positive cells in gene trapped mice (E). In addition, we observed fewer B cells positive for B220 and MHC class II in the gene trapped mice (F). The plasma IgG3 levels were reduced in female homozygously gene trapped mice (G) and IgG1 levels were reduced in male gene trapped mice (H). In contrast we found elevated corticosterone levels in male and female gene trapped mice (I). The data are presented as box plot with strip charts showing the individual animals split by sex and genotype. Female mice are shown as filled circles and males as diamonds. The box represents the 25% and 75% quartile and the line within the boxplot represents the median. The asterisk represents the mean. Circled points or diamonds denote values outside 1.5× the interquartile range. F.con: female $Ftsj1^{+/-}$ mice (n = 15); f.mut: female $Ftsj1^{-/-}$ mice (n = 10); m.con: male $Ftsj1^{+/y}$ mice (n = 14); m.mut: male $Ftsj1^{-/y}$ mice (n = 12). Data were analyzed using a linear regression model.

category were “Plasminogen activation” (p = 1.1E−6) and “Blood coagulation” (p = 3.1E−5) for BP, “Blood microparticle” (p = 1.3E−13) and “Extracellular space” (p = 2.4E−12) for CC, and “Phospholipid binding” (1.5E−6) and “lipid binding” (2.8E−5) for MF (Supplementary Table 3). A search for genes enriched in KEGG Pathway database revealed enrichment for genes belonging to the pathways “complement and coagulation cascades” (p = 4.2E−2), “platelet activation” (p = 9.8E−2) and “fat digestion and absorption” (p = 6.7E−2) (Supplementary Table 4).

Of 50 differentially expressed genes 11 are not coding for proteins. Two of these encode miRNAs and eight encode snoRNAs. snoRNAs are RNAs that either mediate or are predicted to mediate site-specific 2′-*O*-methylation or pseudouridinylation of 18S, 28S, 5.8S rRNAs and the U6 spliceosomal RNA [25]. In addition, we found enhanced expression of *Gas5*, which is upregulated in nutrient-deprived cells and contains a glucocorticoid response element. Expression levels in each of the three litter mates are shown in Supplementary Table 5.

3.7. Patient reexamination

Based on the phenotypic features found in Ftsj1 deficient mice the mutation carriers from two previously published families A003 and MRX9 were re-examined. As *FTSJ1* related ID is categorized as non-syndromic, we did not expect to find consistent alterations, but we did observe individual alterations related to cholesterol levels, muscle strength, hypoalgesia, hematology, triglyceride and hormone levels (summarized in Table 3) in patients or the female carrier, which strongly suggest that the effects of *FTSJ1* deficiency are not restricted to cognitive features in humans either.

4. Discussion

We report here on the generation and characterization of a mouse model for *Ftsj1* deficiency and show that *Ftsj1* deficiency is not restricted to cognitive features but affects the entire organism. The *Ftsj1* gene trapped mice show a mild learning/memory phenotype only, whereas human male patients are also moderately or severely affected. Since the male mice were almost a year old at the time of testing more experiments using mice of different age are required to investigate this impairment in detail. We observed pronounced differences between hemizygous male mutation carriers and male controls. We also saw differences between heterozygous and homozygous females, albeit less pronounced, suggesting that heterozygous female mice are not entirely unaffected. This is surprising, as human heterozygous females seem

Table 2
Mean RNA expression level and fold change in the brains of three Ftsj1 gene trapped and three wild type littermates.

Symbol	Ftsj1 −/y	Ftsj1 +/y	Fold change	Adjusted p-value	Description
Alb	620,57	17,86	34,74	5,05E−141	Albumin
Apob	195,29	11,56	16,89	1,20E−46	Apolipoprotein B
Ftsj1	26,96	152,18	0,18	7,68E−20	Ftsj1
Serpina3k	48,65	0,99	49,21	1,92E−15	Serine protease inhibitor A3K precursor
Mup3	38,33	0,00	Inf	2,04E−14	Major urinary protein 3
Pzp	52,32	3,31	15,83	1,62E−12	Pregnancy zone protein
Gc	51,31	3,63	14,12	9,77E−12	Group specific component
Fgg	34,65	0,99	34,86	5,46E−10	Fibrinogen Gamma Chain
Apoa1	45,97	4,63	9,93	9,85E−09	Apolipoprotein A-I
Cyp3a11	41,32	3,64	11,37	2,44E−08	Cytochrome P450, family 3, subfamily a, polypeptide 11
Fga	32,65	1,99	16,44	1,73E−07	Fibrinogen alpha chain
Gas5	8811,21	5710,96	1,54	2,00E−07	Growth Arrest Specific 5 (Non-Protein Coding)
Snora16a	815,61	474,92	1,72	2,10E−07	Small Nucleolar RNA, H/ACA Box 16A
Mug1	21,33	0,00	Inf	2,89E−07	Murinoglobulin 1
Doc2g	73,89	173,61	0,43	1,18E−06	Double C2, gamma
Apoa2	40,99	5,63	7,28	2,31E−06	Apolipoprotein A-II
Snord22	2958,36	1948,18	1,52	4,22E−06	Small Nucleolar RNA, C/D Box 22
Cps1	42,64	7,29	5,85	1,40E−05	Carbamoyl Phosphate Synthase
Capn11	30,62	3,31	9,25	2,69E−05	Calpain 11
Akr1c6	15,33	0,00	Inf	1,09E−04	Aldo-keto reductase family 1, member C6
Omp	6,32	35,35	0,18	3,14E−04	Olfactory Marker Protein
Slco1b2	26,99	3,30	8,17	3,99E−04	Solute carrier organic anion transporter family, member 1b2
Ahsg	22,66	1,98	11,43	4,48E−04	Alpha-2-HS-glycoprotein
Fgb	23,99	2,65	9,05	8,14E−04	Fibrinogen beta chain
Pigr	14,66	0,33	44,14	1,43E−03	Polymeric Immunoglobulin Receptor
Snord96a	255,96	148,92	1,72	1,81E−03	Small Nucleolar RNA, C/D Box 96A
Azgp1	14,32	0,33	43,27	1,84E−03	Alpha-2-glycoprotein 1, zinc
Fabp1	21,66	2,32	9,35	2,00E−03	Fatty acid binding protein 1, liver
Snora28	935,71	644,67	1,45	2,59E−03	Small Nucleolar RNA, H/ACA Box 28
Col1a1	254,25	150,18	1,69	2,97E−03	Collagen, type 1, alpha 1
Snord15b	1621,55	1153,96	1,41	3,07E−03	Small Nucleolar RNA, C/D Box 14b (Snord 15b)
Mir5117	928,18	644,19	1,44	3,74E−03	MicroRNA 5117
Rgn	21,32	2,65	8,05	4,80E−03	Regucalcin
Hpd	12,98	0,33	39,10	5,50E−03	4-Hydroxyphenylpyruvic acid dioxygenase
C3	67,62	26,50	2,55	5,56E−03	Complement Component 3
Hpx	22,99	3,64	6,32	9,33E−03	Hemopexin
Mir145a	0,33	12,25	0,03	1,07E−02	MicroRNA 145a
Aldob	52,29	18,52	2,82	1,07E−02	Aldolase B, fructose-bisphosphate
Eps8l1	68,92	28,46	2,42	1,07E−02	EPS8-like 1
Ugt2b1	17,33	1,98	8,75	2,05E−02	UDP glucuronosyltransferase 2 family, polypeptide B1
Tor2a	116,15	194,21	0,60	2,16E−02	Torsin Family 2, Member A
Car3	31,32	8,26	3,79	2,76E−02	Carbonic anhydrase 3
Mup20	9,33	0,00	Inf	2,89E−02	Major urinary protein 20
Snord66	189,74	115,19	1,65	3,57E−02	Small Nucleolar RNA, C/D Box 66
Snord67	634,48	451,26	1,41	3,64E−02	Small Nucleolar RNA, C/D Box 67
Serpinh1	302,56	199,10	1,52	3,69E−02	Serin Peptidase Inhibitor H1
Snord87	1003,32	735,87	1,36	3,75E−02	Small Nucleolar RNA, C/D Box 87
Gabra6	729,60	526,65	1,39	3,88E−02	Gamma-aminobutyric acid (GABA) A receptor, subunit alpha 6
Lhx1	60,60	26,16	2,32	4,81E−02	LIM Homeobox Protein 1
Apoh	15,00	1,66	9,04	4,91E−02	Apolipoprotein H

Expression values are given in reads per kilobase per million mapped reads (RPKM).

largely unaffected by *FTSJ1* mutations [18]. Still, as the *Ftsj1* expression pattern in female heterozygous mice is not clear we focused on the effects in male mice where the differences are more pronounced. The gene trapped mice are smaller than wild type littermates but have no organ abnormalities when correcting for the lower body weight. However, the reduced bone mass observed in the gene trapped mice suggests an altered bone metabolism. This is probably related to the reduced calcium levels and the increased alkaline phosphatase activity we observed in the blood of gene trapped mice.

In red blood cells of gene trap carriers, we observed mild microcytosis and increased anisocytosis, which could be related to the lower iron levels we also observed. The effect is significant but not very pronounced as the hemoglobin levels were similar between gene trapped mice and controls. The platelet number was slightly reduced, which could indicate an impaired thrombopoiesis. We also found an increased number of leukocytes, but no signs of allergy or an autoimmune response.

Although we did not observe altered energy metabolism or body temperature, the mutant mice have reduced blood glucose levels and clear intraperitoneally injected glucose faster than controls. Interestingly, patients with mutations in the tRNA modifying enzyme TRMT10A (MIM616033) present with ID, short stature and an abnormal glucose metabolism related to abnormal insulin levels [9,10]. These patients also have reduced blood sugar levels but, in contrast to *Ftsj1* gene trapped mice, clear externally given glucose inefficiently, even though they have normal cortisol levels [10].

The *Ftsj1* gene trapped mice also have decreased levels of alpha-amylase, cholesterol, triglycerides and creatinine, which is indicative of an altered energy metabolism. We also observed a relative increase in body fat content and reduction in lean mass. However, we found no alterations in lactate levels or in oxygen consumption, suggesting normal mitochondrial oxidative capacity.

Of the three investigated hormones (testosterone, aldosterone and corticosterone) corticosterone showed significant upregulation.

Table 3
Clinical investigation of ID patients with mutation in *FTSJ1*.

	Family A003			MRX9		
	Index patient 1848	Affected older brother 1894	Mother carrier 1751	Index patient	Affected uncle	Mother carrier
Intellectual disability	Moderate	Mild	None	Moderate	Mild	None
Cholesterol	4.6 (3.5–5.5)	4 (3.5–5.5)	7.2 (3.5–5.5)	134 (150–190)	197 (< 190)	176 (< 190)
LDL-cholesterol	2.9 (< 3.5)	2.3 (< 3.5)	4.9 (< 3.5)	Normal	117 (< 115)	88 (< 115)
HDL-cholesterol	1.46 (> 1)	1 (> 1)	1.63 (> 1)	Normal	69 (> 41)	75 (> 45)
Impaired muscle strength	Yes	Yes	Not investigated	No	Not investigated	No
Hypoalgesia	Yes	No	Not investigated	Yes	Yes	No
Granulocytes elevated	No	No		yes	no	no
Neutrophil	2.4 (2.0–7.5)	2.4 (2.0–7.5)	1.9 (2.0–7.5)	45% (50–70)	40.1 (38.9–74.9)	
Eosinophil	Not investigated	Not investigated	Not investigated	17% (0–5%)	5.3 (0–5%)	3.2% (0–5%)
Triglyceride (S Trig)	0.6 (< 1.5)	1.6 (< 1.5)	1.5 (< 1.5)	normal	56 (< 150)	64 (< 150)
Estimated glomerular filtration rate (egfr)	Normal	Normal	Normal	Normal	Normal	Normal
Glucose levels (Fasting)	5.5 (3.6–6.0)	5.3 (3.6–6.0)	6.8 (3.6–6.0)	72(55–115)	84 (82–109)	85 (70–100)
Bicarbonate	21 (20 − 32)	33 (20–32)	29 (20–32)	Not investigated	28 (22 − 33)	25
Creatine	50 (60–110)	58 (60–110)	61 (60–110)	0.7 (0.70–1.20)	0.65 (0.5–1.2)	0.9 (< 1.10)
Aspartate aminotransferase	16 (10–40)	9 (10–40)	21 (10–40)	22 (0–35)	16 (< 40)	29 (< 31)
Amylase	Not investigated	19 (20–100)	56 (20–100)	Not investigated	52 (29–100)	71 (< 125)
Testosterone	Not investigated	Not investigated	Not investigated	1044 (200–800)	19.17 (8.64–29)	31.9 (11.0–57.0)
Sexual hormone binding globulin (SHBG)	Not investigated	Not investigated	Not investigated	1.8 (0.3–1.5)	41 (20.6–76.7)	75 (20–155)

Corticosterone belongs to the glucocorticoids, which are important regulators of bone metabolism, energy metabolism and the immune system. It is the major glucocorticoid in mice, whereas the major glucocorticoid in humans is cortisol. It is therefore tempting to speculate that the reduced body size, bone phenotype, altered glucose and fat metabolism as well as the immune system phenotype are related to the elevated corticosterone levels we observed in the gene trapped mice. Still, further investigations are required to elucidate such putatively specific effects in gene trapped mice as the phenotype varies between individuals.

Corticosterone is also a stress related hormone that is known to influence murine learning and memory [26]. In a Rett syndrome (MIM 312750) mouse model a stronger corticosterone response to a stress stimulus was observed when compared to controls [27]. However, as *Ftsj1* gene trapped mice show more explorative behaviour as compared to controls, there is no suggestion of Ftsj1-deficiency related anxiety or any other stress related phenotype.

The hypoalgesic phenotype we observed in mutant animals suggests that also the peripheral nervous system is affected by the absence of functional Ftsj1. Interestingly, an increased pain threshold has also been observed in ID patients with Prader-Willi syndrome (MIM 176270) [28] or Rett syndrome [29]. In Children with Prader-Willi syndrome, for example, the higher pain threshold has been related to the increased serum neurotensin levels [28] and in a zebrafish model for Rett syndrome knock-down of mecp2 leads to an impaired sensory system due to defects in peripheral innervation of trigeminal sensory neurons [30]. Moreover, reduced pain sensitivity is also observed in familial dysautonomia (FD, MIM 223900) patients that harbor a splice-site mutation in *IKBKAP/ELP1* [31,32]. *IKBKAP/ELP1* encodes a subunit of the Elongator complex, which is required for modifying uridine at the wobble position in certain tRNAs, highlighting the importance for proper tRNA modifications in nervous system cells.

The mouse model expresses no detectable wild type transcript and truncated forms are found at a reduced level. A similarly reduced expression level has also been reported for most of the ID patients where truncating mutations have been found [15,16,18]. Although the presence of a truncated Ftsj1 protein in our mice cannot be entirely excluded, such a putative protein would still lack half of the amino acids and one third of the conserved methyltransferase domain and thus still be dysfunctional. Two seemingly less severe mutations have been reported in ID patients with *FTSJ1* mutations. One mutation (c.655G > A) leads to skipping of exon 9 without affecting the *FTSJ1* mRNA expression level [15] and a splice-site mutation in intron 8 (c.571 + 1 G > A), leading to a frameshift, was shown to cause premature termination in exon 9 as well as reduced *FTSJ1* mRNA levels [18]. Moreover, the ExAC or gnomAD databases contain no loss-of-function entries for this gene. These observations further corroborate our conclusion that premature termination of the protein abolishes its enzymatic activity.

The RNA expression profile of our model showed significantly altered expression levels of 50 genes, most of them being upregulated in the gene trapped mouse brain tissue. By applying the DAVID functional annotation software [23] to the 50 genes, we found enrichment for genes included in the GO term “blood microparticle” (GO:0072562). Blood microparticles are phospholipid microvesicles that contain receptors and other protein characteristics of the parental cell. Elevated microparticle levels have been found in the cerebrospinal fluid of Alzheimer disease patients together with increased Calpain activity [33] which is interesting as we found *Capn11* significantly upregulated in *Ftsj1* deficient mouse brain tissue. Differentially expressed genes were also enriched in the KEGG pathways “Complement and coagulation cascade” and “platelet activation” supporting an effect on microparticles in Ftsj1 deficient mice. However, further investigations are necessary to show if Ftsj1$^{-/y}$ mice actually contain more blood microparticles than controls.

We also found modest upregulation of non-coding RNAs including the long non-coding RNA gene *Gas5* (Growth arrest-specific 5), and several snoRNAs. *Gas5* shows higher expression in growth-arrested cells [34] as well as in lysine deprived cells [35]. This suggests that Ftsj1 deficient mouse brain cells activate an amino acid starvation response as it has been shown for *Trm7* deficient yeast cells [37]. The *Gas5* transcript contains a glucocorticoid-binding motif in the 3′ end, which is able to mimic the glucocorticoid response element. The binding of *Gas5* transcript to the glucocorticoid receptor (GR) leads to inactivation of GR, which is then no longer able to activate transcription [36]. The elevated corticosterone levels observed in the blood of gene trapped mice furthermore suggest that the active GR levels are balanced with the elevated Gas5 levels because we did not observe differential expression of other GR regulated genes than *Gas5* [38].

Eight of 50 deregulated genes encode snoRNAs involved in site specific modifications of ribosomal RNA molecules (5.8S, 18S and 28S rRNA) and the U6 spliceosomal RNA. snoRNAs containing an H/ACA box are involved in the conversion of uridine to pseudouridine [39] and CD box containing snoRNAs guide 2′-*O*-methylation [40]. Yeast *Trm7* and human *FTSJ1* deficient cells contain hypo-methylated tRNA^{Phe} [19], which is most likely also the case for the gene trapped mouse

brain cells. Upregulation of snoRNA genes in the gene trapped cells could suggest the presence of a feedback mechanism that is activated in response to the presence of hypomethylated tRNAs. Two tRNA quality control mechanisms have been described that eventually either degrade pre-tRNAs lacking 1-methyladenosine [41] or degrade mature hypomodified tRNAs through the rapid tRNA decay pathway [42]. Cleavage of tRNAs in response to cellular stress has also been reported for *Nsun2* deficient mice [43]. However, further experiments are required to determine the fate of hypomethylated $tRNA^{Phe}$ in Ftsj1 deficient nerve cells.

Mutations in *FTSJ1* mainly give rise to intellectual disability but a re-investigation of patients from two families (A003 and MRX9) showed that several features present in individual patients also could be observed in some of the gene trapped mice. Phenotypic variability seems to be pronounced in both human and mice with mutated *FTSJ1/Ftsj1*. However, the phenotypic variability is not caused by differences in the genetic background or from different treatment of the mice as the mice are essentially identical, born within the same week and fed and treated the same way.

That impaired protein synthesis probably is the key to understand the effects of FTSJ1 deficiency in mouse and man is in line with recent findings of mutations in aminoacyl-tRNA synthetase genes in ID patients. Mutations have been reported for *SARS* and *WARS2* [44], *PARS2* and *NARS2* [45], *IARS* [46] and *RARS2* [47] and in *AIMP1*, which encodes a part of a complex that ligates amino acids to their respective tRNA [48]. Furthermore, yeast cells deficient for the *Ftsj1* homologue *Trm7* show a severe growth defect and impaired translation [20]. This is also in line with the lower total protein levels we observed in blood from the gene trapped mice.

FTSJ1 is ubiquitously expressed, but only causing non-syndromic ID when mutated as other clinical manifestations are inconsistent. However, an increased pain threshold was found in the gene trapped mice and in affected individuals from both investigated ID families and may be a feature that is more common in patients with FTSJ1 deficiency. Why mutations in this evolutionarily old protein lead to a restricted phenotype in human and mice is still an open question. As FTSJ1 deficiency is not lethal it is possible that evolutionarily comparatively young features like human cognition may be more severely affected than other tissues because the brain has not had the time to develop proper back-up mechanisms to compensate for FTSJ1 deficiency. The Ftsj1 gene trapped mice will be a suitable model for addressing the different effects of disturbed protein synthesis in different mammalian tissues and answering the question as to why the central and peripheral nervous systems are more sensitive than other organs.

In conclusion, we have generated and thoroughly characterized a mouse model for non-syndromic intellectual disability. The *Ftsj1* deficient mice are small and have cognitive deficits and altered bone and energy metabolism. Muscle strength and pain sensing is reduced and the immune system and the hormone system is also affected. Some of these features were found upon re-examination of ID patients with *FTSJ1* mutations, though too few ID families with *FTSJ1* mutations have been identified to define a syndrome. Functional enrichment of differentially expressed mRNAs suggests involvement of blood microparticles and coagulation factors in brains of mice with defective *Ftsj1*.

Supplementary data to this article can be found online at https://doi.org/10.1016/j.bbadis.2018.12.011.

Transparency document

The Transparency document associated with this article can be found, in online version.

Acknowledgement

We thank the patients and their families for their participation in the study. We also thank Bettina Lipkowitz, Marion Amende and the technicians at the animal facility at the Max Planck Institute for Molecular genetics, the GMC technicians as well as the GMC animal caretaker team for excellent technical assistance. We thank Robert Weissmann for help with the bioinformatic analysis.

Funding

This work was supported by the German Federal Ministry of Education and Research [Infrafrontier grant 01KX1012 to MHdA] and through the Integrated Network IntegraMent (Integrated Understanding of Causes and Mechanisms in Mental Disorders), under the auspices of the e:Med Programme [grant 01ZX1314H to W. Wurst], by the German Science Foundation Collaborative Research Centre (CRC) 870 and by the Helmholtz Portfolio Theme ‘Supercomputing and Modelling for the Human Brain’ (SMHB).

Conflict of interest statement

None declared.

References

[1] P.K. Maulik, M.N. Mascarenhas, C.D. Mathers, T. Dua, S. Saxena, Prevalence of intellectual disability: a meta-analysis of population-based studies, Res. Dev. Disabil. 32 (2011) 419–436, https://doi.org/10.1016/j.ridd.2010.12.018.
[2] P. Chiurazzi, F. Pirozzi, Advances in understanding - genetic basis of intellectual disability, F1000Res 5 (2016), https://doi.org/10.12688/f1000research.7134.1.
[3] H. Najmabadi, H. Hu, M. Garshasbi, T. Zemojtel, S.S. Abedini, W. Chen, M. Hosseini, F. Behjati, S. Haas, P. Jamali, et al., Deep sequencing reveals 50 novel genes for recessive cognitive disorders, Nature 478 (2011) 57–63, https://doi.org/10.1038/nature10423.
[4] C. Gilissen, J.Y. Hehir-Kwa, D.T. Thung, M. van de Vorst, B.W.M. van Bon, M.H. Willemsen, M. Kwint, I.M. Janssen, A. Hoischen, A. Schenck, et al., Genome sequencing identifies major causes of severe intellectual disability, Nature 511 (2014) 344–347, https://doi.org/10.1038/nature13394.
[5] L. Abbasi-Moheb, S. Mertel, M. Gonsior, L. Nouri-Vahid, K. Kahrizi, S. Cirak, D. Wieczorek, M.M. Motazacker, S. Esmaeeli-Nieh, K. Cremer, et al., Mutations in NSUN2 cause autosomal-recessive intellectual disability, Am. J. Hum. Genet. 90 (2012) 847–855, https://doi.org/10.1016/j.ajhg.2012.03.021.
[6] M.A. Khan, M.A. Rafiq, A. Noor, S. Hussain, J.V. Flores, V. Rupp, A.K. Vincent, R. Malli, G. Ali, F.S. Khan, et al., Mutation in NSUN2, which encodes an RNA methyltransferase, causes autosomal-recessive intellectual disability, Am. J. Hum. Genet. 90 (2012) 856–863, https://doi.org/10.1016/j.ajhg.2012.03.023.
[7] F.J. Martinez, J.H. Lee, J.E. Lee, S. Blanco, E. Nickerson, S. Gabriel, M. Frye, L. Al-Gazali, J.G. Gleeson, Whole exome sequencing identifies a splicing mutation in NSUN2 as a cause of a Dubowitz-like syndrome, J. Med. Genet. 49 (2012) 380–385, https://doi.org/10.1136/jmedgenet-2011-100686.
[8] A.M. Alazami, H. Hijazi, M.S. Al-Dosari, R. Shaheen, A. Hashem, M.A. Aldahmesh, J.Y. Mohamed, A. Kentab, M.A. Salih, A. Awaji, et al., Mutation in ADAT3, encoding adenosine deaminase acting on transfer RNA, causes intellectual disability and strabismus, J. Med. Genet. 50 (2013) 425–430, https://doi.org/10.1136/jmedgenet-2012-101378.
[9] M. Igoillo-Esteve, A. Genin, N. Lambert, J. Desir, I. Pirson, B. Abdulkarim, N. Simonis, A. Drielsma, L. Marselli, P. Marchetti, et al., tRNA methyltransferase homolog gene TRMT10A mutation in young onset diabetes and primary microcephaly in humans, PLoS Genet. 9 (2013) e1003888, , https://doi.org/10.1371/journal.pgen.1003888.
[10] D. Gillis, A. Krishnamohan, B. Yaacov, A. Shaag, J.E. Jackman, O. Elpeleg, TRMT10A dysfunction is associated with abnormalities in glucose homeostasis, short stature and microcephaly, J. Med. Genet. 51 (2014) 581–586, https://doi.org/10.1136/jmedgenet-2014-102282.
[11] J.W. Yarham, T.N. Lamichhane, A. Pyle, S. Mattijssen, E. Baruffini, F. Bruni, C. Donnini, A. Vassilev, L. He, E.L. Blakely, et al., Defective i6A37 modification of mitochondrial and cytosolic tRNAs results from pathogenic mutations in TRIT1 and its substrate tRNA, PLoS Genet. 10 (2014) e1004424, , https://doi.org/10.1371/journal.pgen.1004424.
[12] J.S. Cohen, S. Srivastava, K.D. Farwell, H.-M. Lu, W. Zeng, H. Lu, E.C. Chao, A. Fatemi, ELP2 is a novel gene implicated in neurodevelopmental disabilities, Am. J. Med. Genet. A 167 (2015) 1391–1395, https://doi.org/10.1002/ajmg.a.36935.
[13] R. Shaheen, L. Han, E. Faqeih, N. Ewida, E. Alobeid, E.M. Phizicky, F.S. Alkuraya, A homozygous truncating mutation in PUS3 expands the role of tRNA modification in normal cognition, Hum. Genet. 135 (2016) 707–713, https://doi.org/10.1007/s00439-016-1665-7.
[14] M. Charif, S.M.C. Titah, A. Roubertie, V. Desquiret-Dumas, N. Gueguen, I. Meunier, J. Leid, F. Massal, X. Zanlonghi, J. Mercier, et al., Optic neuropathy, cardiomyopathy, cognitive disability in patients with a homozygous mutation in the nuclear MTO1 and a mitochondrial MT-TF variant, Am. J. Med. Genet. A 167A (2015) 2366–2374, https://doi.org/10.1002/ajmg.a.37188.
[15] K. Freude, K. Hoffmann, L.-R. Jensen, M.B. Delatycki, V. Des Portes, B. Moser,

B. Hamel, H. van Bokhoven, C. Moraine, J.-P. Fryns, et al., Mutations in the FTSJ1 gene coding for a novel S-adenosylmethionine-binding protein cause nonsyndromic X-linked mental retardation, Am. J. Hum. Genet. 75 (2004) 305–309, https://doi.org/10.1086/422507.
[16] J. Ramser, B. Winnepenninckx, C. Lenski, V. Errijgers, M. Platzer, C.E. Schwartz, A. Meindl, R.F. Kooy, A splice site mutation in the methyltransferase gene FTSJ1 in Xp11.23 is associated with non-syndromic mental retardation in a large Belgian family (MRX9), J. Med. Genet. 41 (2004) 679–683, https://doi.org/10.1136/jmg.2004.019000.
[17] G. Froyen, M. Bauters, J. Boyle, H. van Esch, K. Govaerts, H. van Bokhoven, H.-H. Ropers, C. Moraine, J. Chelly, J.-P. Fryns, et al., Loss of SLC38A5 and FTSJ1 at Xp11.23 in three brothers with non-syndromic mental retardation due to a microdeletion in an unstable genomic region, Hum. Genet. 121 (2007) 539–547, https://doi.org/10.1007/s00439-007-0343-1.
[18] K. Takano, E. Nakagawa, K. Inoue, F. Kamada, S. Kure, Y.-i. Goto, A loss-of-function mutation in the FTSJ1 gene causes nonsyndromic X-linked mental retardation in a Japanese family, Am. J. Med. Genet. B Neuropsychiatr. Genet. 147B (2008) 479–484, https://doi.org/10.1002/ajmg.b.30638.
[19] M.P. Guy, M. Shaw, C.L. Weiner, L. Hobson, Z. Stark, K. Rose, V.M. Kalscheuer, J. Gecz, E.M. Phizicky, Defects in tRNA anticodon loop 2′-*O*-methylation are implicated in nonsyndromic X-linked intellectual disability due to mutations in FTSJ1, Hum. Mutat. 36 (2015) 1176–1187, https://doi.org/10.1002/humu.22897.
[20] L. Pintard, F. Lecointe, J.M. Bujnicki, C. Bonnerot, H. Grosjean, B. Lapeyre, Trm7p catalyses the formation of two 2′-*O*-methylriboses in yeast tRNA anticodon loop, EMBO J. 21 (2002) 1811–1820, https://doi.org/10.1093/emboj/21.7.1811.
[21] M.P. Guy, E.M. Phizicky, Conservation of an intricate circuit for crucial modifications of the tRNAPhe anticodon loop in eukaryotes, RNA 21 (2015) 61–74, https://doi.org/10.1261/rna.047639.114.
[22] M.P. Guy, B.M. Podyma, M.A. Preston, H.H. Shaheen, K.L. Krivos, P.A. Limbach, A.K. Hopper, E.M. Phizicky, Yeast Trm7 interacts with distinct proteins for critical modifications of the tRNAPhe anticodon loop, RNA 18 (2012) 1921–1933, https://doi.org/10.1261/rna.035287.112.
[23] D.W. Huang, B.T. Sherman, R.A. Lempicki, Systematic and integrative analysis of large gene lists using DAVID bioinformatics resources, Nat. Protoc. 4 (2009) 44–57, https://doi.org/10.1038/nprot.2008.211.
[24] D.W. Huang, B.T. Sherman, R.A. Lempicki, Bioinformatics enrichment tools: paths toward the comprehensive functional analysis of large gene lists, Nucleic Acids Res. 37 (2009) 1–13, https://doi.org/10.1093/nar/gkn923.
[25] L. Lestrade, M.J. Weber, snoRNA-LBME-db, a comprehensive database of human H/ACA and C/D box snoRNAs, Nucleic Acids Res. 34 (2006) D158–D162, https://doi.org/10.1093/nar/gkj002.
[26] O. Wiegert, M. Joels, H. Krugers, Timing is essential for rapid effects of corticosterone on synaptic potentiation in the mouse hippocampus, Learn. Mem. 13 (2006) 110–113, https://doi.org/10.1101/lm.87706.
[27] B.E. McGill, S.F. Bundle, M.B. Yaylaoglu, J.P. Carson, C. Thaller, H.Y. Zoghbi, Enhanced anxiety and stress-induced corticosterone release are associated with increased Crh expression in a mouse model of Rett syndrome, Proc. Natl. Acad. Sci. U. S. A. 103 (2006) 18267–18272, https://doi.org/10.1073/pnas.0608702103.
[28] M.G. Butler, T.A. Nelson, D.J. Driscoll, A.M. Manzardo, High plasma neurotensin levels in children with Prader-Willi syndrome, Am. J. Med. Genet. A 167A (2015) 1773–1778, https://doi.org/10.1002/ajmg.a.37103.
[29] R.C. Samaco, J.D. Fryer, J. Ren, S. Fyffe, H.-T. Chao, Y. Sun, J.J. Greer, H.Y. Zoghbi, J.L. Neul, A partial loss of function allele of methyl-CpG-binding protein 2 predicts a human neurodevelopmental syndrome, Hum. Mol. Genet. 17 (2008) 1718–1727, https://doi.org/10.1093/hmg/ddn062.
[30] W.Y. Leong, Z.H. Lim, V. Korzh, T. Pietri, E.L.K. Goh, Methyl-CpG binding protein 2 (Mecp2) regulates sensory function through Sema5b and Robo2, Front. Cell. Neurosci. 9 (2015) 481, https://doi.org/10.3389/fncel.2015.00481.
[31] S.L. Anderson, R. Coli, I.W. Daly, E.A. Kichula, M.J. Rork, S.A. Volpi, J. Ekstein, B.Y. Rubin, Familial dysautonomia is caused by mutations of the IKAP gene, Am. J. Hum. Genet. 68 (2001) 753–758, https://doi.org/10.1086/318808.
[32] S.A. Slaugenhaupt, A. Blumenfeld, S.P. Gill, M. Leyne, J. Mull, M.P. Cuajungco, C.B. Liebert, B. Chadwick, M. Idelson, L. Reznik, et al., Tissue-specific expression of a splicing mutation in the IKBKAP gene causes familial dysautonomia, Am. J. Hum. Genet. 68 (2001) 598–605.
[33] C. Laske, K. Stellos, I. Kempter, E. Stransky, W. Maetzler, I. Fleming, V. Randriamboavonjy, Increased cerebrospinal fluid calpain activity and microparticle levels in Alzheimer's disease, Alzheimers Dement. 11 (2015) 465–474, https://doi.org/10.1016/j.jalz.2014.06.003.
[34] T. Mayama, A.K. Marr, T. Kino, Differential expression of glucocorticoid receptor noncoding RNA repressor Gas5 in autoimmune and inflammatory diseases, Horm. Metab. Res. 48 (2016) 550–557, https://doi.org/10.1055/s-0042-106898.
[35] N. Fontanier-Razzaq, D.N. Harries, S.M. Hay, W.D. Rees, Amino acid deficiency up-regulates specific mRNAs in murine embryonic cells, J. Nutr. 132 (2002) 2137–2142.
[36] T. Kino, D.E. Hurt, T. Ichijo, N. Nader, G.P. Chrousos, Noncoding RNA gas5 is a growth arrest- and starvation-associated repressor of the glucocorticoid receptor, Sci. Signal. 3 (2010) ra8, , https://doi.org/10.1126/scisignal.2000568.
[37] L. Han, M.P. Guy, Y. Kon, E.M. Phizicky, Lack of 2′-*O*-methylation in the tRNA anticodon loop of two phylogenetically distant yeast species activates the general amino acid control pathway, PLoS Genet. 14 (2018) e1007288, , https://doi.org/10.1371/journal.pgen.1007288.
[38] P. Phuc Le, J.R. Friedman, J. Schug, J.E. Brestelli, J.B. Parker, I.M. Bochkis, K.H. Kaestner, Glucocorticoid receptor-dependent gene regulatory networks, PLoS Genet. 1 (2005) e16, https://doi.org/10.1371/journal.pgen.0010016.
[39] P. Ganot, M.L. Bortolin, T. Kiss, Site-specific pseudouridine formation in preribosomal RNA is guided by small nucleolar RNAs, Cell 89 (1997) 799–809.
[40] Z. Kiss-Laszlo, Y. Henry, J.P. Bachellerie, M. Caizergues-Ferrer, T. Kiss, Site-specific ribose methylation of preribosomal RNA: a novel function for small nucleolar RNAs, Cell 85 (1996) 1077–1088.
[41] S. Kadaba, X. Wang, J.T. Anderson, Nuclear RNA surveillance in Saccharomyces cerevisiae: Trf4p-dependent polyadenylation of nascent hypomethylated tRNA and an aberrant form of 5S rRNA, RNA 12 (2006) 508–521, https://doi.org/10.1261/rna.2305406.
[42] A. Alexandrov, I. Chernyakov, W. Gu, S.L. Hiley, T.R. Hughes, E.J. Grayhack, E.M. Phizicky, Rapid tRNA decay can result from lack of nonessential modifications, Mol. Cell 21 (2006) 87–96, https://doi.org/10.1016/j.molcel.2005.10.036.
[43] S. Blanco, S. Dietmann, J.V. Flores, S. Hussain, C. Kutter, P. Humphreys, M. Lukk, P. Lombard, L. Treps, M. Popis, et al., Aberrant methylation of tRNAs links cellular stress to neuro-developmental disorders, EMBO J. 33 (2014) 2020–2039, https://doi.org/10.15252/embj.201489282.
[44] L. Musante, L. Puttmann, K. Kahrizi, M. Garshasbi, H. Hu, H. Stehr, B. Lipkowitz, S. Otto, L.R. Jensen, A. Tzschach, et al., Mutations of the aminoacyl-tRNA-synthetases SARS and WARS2 are implicated in the etiology of autosomal recessive intellectual disability, Hum. Mutat. (2017), https://doi.org/10.1002/humu.23205.
[45] T. Mizuguchi, M. Nakashima, M. Kato, K. Yamada, T. Okanishi, N. Ekhilevitch, H. Mandel, A. Eran, M. Toyono, Y. Sawaishi, et al., PARS2 and NARS2 mutations in infantile-onset neurodegenerative disorder, J. Hum. Genet. (2017), https://doi.org/10.1038/jhg.2016.163.
[46] R. Kopajtich, K. Murayama, A.R. Janecke, T.B. Haack, M. Breuer, A.S. Knisely, I. Harting, T. Ohashi, Y. Okazaki, D. Watanabe, et al., Biallelic IARS mutations cause growth retardation with prenatal onset, intellectual disability, muscular hypotonia, and infantile hepatopathy, Am. J. Hum. Genet. 99 (2016) 414–422, https://doi.org/10.1016/j.ajhg.2016.05.027.
[47] D. Cassandrini, M.R. Cilio, M. Bianchi, M. Doimo, M. Balestri, A. Tessa, T. Rizza, G. Sartori, M.C. Meschini, C. Nesti, et al., Pontocerebellar hypoplasia type 6 caused by mutations in RARS2: definition of the clinical spectrum and molecular findings in five patients, J. Inherit. Metab. Dis. 36 (2013) 43–53, https://doi.org/10.1007/s10545-012-9487-9.
[48] Z. Iqbal, L. Puttmann, L. Musante, A. Razzaq, M.Y. Zahoor, H. Hu, T.F. Wienker, M. Garshasbi, Z. Fattahi, C. Gilissen, et al., Missense variants in AIMP1 gene are implicated in autosomal recessive intellectual disability without neurodegeneration, Eur. J. Hum. Genet. 24 (2016) 392–399, https://doi.org/10.1038/ejhg.2015.148.
[49] G. Longenecker, A.B. Kulkarni, Generation of gene knockout mice by ES cell microinjection, Curr. Protoc. Cell Biol. (2009), https://doi.org/10.1002/0471143030.cb1914s44 (Chapter 19, Unit 19.14 19.14.1-36).
[50] B. Rathkolb, W. Hans, C. Prehn, H. Fuchs, V. Gailus-Durner, B. Aigner, J. Adamski, E. Wolf, M. Hrabe de Angelis, Clinical chemistry and other laboratory tests on mouse plasma or serum, Curr. Protoc. Mouse Biol. 3 (2013) 69–100, https://doi.org/10.1002/9780470942390.mo130043.
[51] V. Gailus-Durner, H. Fuchs, L. Becker, I. Bolle, M. Brielmeier, J. Calzada-Wack, R. Elvert, N. Ehrhardt, C. Dalke, T.J. Franz, et al., Introducing the German Mouse Clinic: open access platform for standardized phenotyping, Nat. Methods 2 (2005) 403–404, https://doi.org/10.1038/nmeth0605-403.
[52] H. Fuchs, V. Gailus-Durner, T. Adler, J.A. Aguilar-Pimentel, L. Becker, J. Calzada-Wack, P. Da Silva-Buttkus, F. Neff, A. Gotz, W. Hans, et al., Mouse phenotyping, Methods 53 (2011) 120–135, https://doi.org/10.1016/j.ymeth.2010.08.006.
[53] S.M. Holter, L. Garrett, J. Einicke, B. Sperling, P. Dirscherl, A. Zimprich, H. Fuchs, V. Gailus-Durner, M. Hrabe de Angelis, W. Wurst, Assessing cognition in mice, Curr. Protoc. Mouse Biol. 5 (2015) 331–358, https://doi.org/10.1002/9780470942390.mo150068.
[54] J. Bertram, L. Koschutzke, J.P. Pfannmoller, J. Esche, L. van Diepen, A.W. Kuss, B. Hartmann, D. Bartsch, M. Lotze, O. von Bohlen Und Halbach, Morphological and behavioral characterization of adult mice deficient for SrGAP3, Cell Tissue Res. 366 (2016) 1–11, https://doi.org/10.1007/s00441-016-2413-y.
[55] Y. Bouter, T. Kacprowski, R. Weissmann, K. Dietrich, H. Borgers, A. Brauss, C. Sperling, O. Wirths, M. Albrecht, L.R. Jensen, et al., Deciphering the molecular profile of plaques, memory decline and neuron loss in two mouse models for Alzheimer's disease by deep sequencing, Front. Aging Neurosci. 6 (2014) 75, , https://doi.org/10.3389/fnagi.2014.00075.
[56] D. Risso, K. Schwartz, G. Sherlock, S. Dudoit, GC-content normalization for RNA-Seq data, BMC Bioinformatics 12 (2011) 480, , https://doi.org/10.1186/1471-2105-12-480.
[57] S. Anders, W. Huber, Differential expression analysis for sequence count data, Genome Biol. 11 (2010) R106, , https://doi.org/10.1186/gb-2010-11-10-r106.

Databases

[other]
DAVID: https://david.ncifcrf.gov/.
[other]
ExAC Browser: http://exac.broadinstitute.org/.
[other]
gnomAD: http://gnomad.broadinstitute.org/.